THE JOURNAL OF PHYSICAL CHEMISTRY LETTERS
A JOURNAL OF THE AMERICAN CHEMICAL SOCIETY

pubs.acs.org/JPCL

Letter

Increasing the Modulation Depth of Gd^{III}-Based Pulsed Dipolar EPR Spectroscopy (PDS) with Porphyrin−Gd^{III} Laser-Induced Magnetic Dipole Spectroscopy

Andreas Scherer, Xuemei Yao, Mian Qi, Max Wiedmaier, Adelheid Godt,* and Malte Drescher*

Cite This: J. Phys. Chem. Lett. 2022, 13, 10958−10964

Read Online

ABSTRACT: Distance determination with pulsed EPR has become an important technique for the structural investigation of biomacromolecules, with double electron−electron resonance spectroscopy (DEER) as the most important method. Gd^{III}-based spin labels are one of the most frequently used spin labels for DEER owing to their stability against reduction, high magnetic moment, and absence of orientation selection. A disadvantage of Gd^{III}−Gd^{III} DEER is the low modulation depth due to the broad EPR spectrum of Gd^{III}. Here, we introduce laser-induced magnetic dipole spectroscopy (LaserIMD) with a spin pair consisting of Gd^{III}(PymiMTA) and a photoexcited porphyrin as an alternative technique. We show that the excited state of the porphyrin is not disturbed by the presence of the Gd^{III} complex and that herewith modulation depths of almost 40% are possible. This is significantly higher than the value of 7.2% that was achieved with Gd^{III}−Gd^{III} DEER.

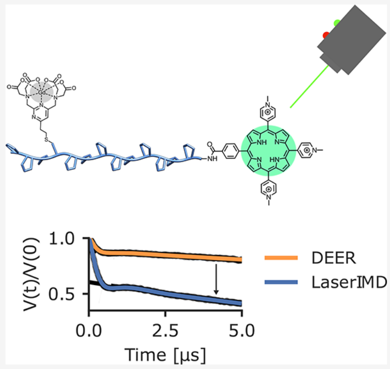

Pulsed dipolar EPR spectroscopy (PDS) has become an important tool for the structural analysis of biomacromolecules like proteins, DNA, and RNA.[1−8] PDS measures the magnetic dipolar coupling ω_{dd} between two paramagnetic centers in frozen solution, from which distance distributions in the nanometer range can be calculated.[9] Among the many techniques that have been developed,[10−13] double electron−electron resonance spectroscopy (DEER) is the most common one.[9,14]

Because biomolecules rarely contain unpaired electrons, PDS requires usually that paramagnetic labels, called spin labels, are attached at defined sites. Although nitroxides and carbon-based trityl labels have received the most attention in the last years,[15−18] Gd^{III} complexes with a chelating ligand (electron spin $S = 7/2$) are becoming increasingly popular.[3,19,20] Their advantages includes reduction stability,[21,22] the absence of orientation selection and high sensitivities at Q- and W-bands.[23−27] However, their broad EPR spectrum spans several GHz and exceeds the excitation bandwidth of most resonators and microwave pulses.[28] Therefore, only a small fraction of spins are addressed by the microwave pump pulse used in Gd^{III}−Gd^{III} DEER, which results in a much lower modulation depth than those achieved with other PDS techniques or labels.[23,26] Another drawback of Gd^{III}−Gd^{III} DEER are broadening artifacts that appear at distances below ≈3 nm if the offset between the observer and pump microwave frequency is in the range of only a few 100 MHz.[29−32] One technique with which both of these disadvantages for Gd^{III}-based PDS can be overcome is relaxation induced dipolar modulation enhancement (RIDME).[33,34] In RIDME, the spin flips of the pump spins take place as stochastic events due to relaxation and are thus not limited by the excitation bandwidth of the microwave pulses.[12,35] Hence, modulation depths higher than 50% are possible with Gd^{III}−Gd^{III} RIDME.[33] However, because spin flips with $\Delta|m_S| > 1$ are also possible, Gd^{III}−Gd^{III} RIDME suffers from the excitation of overtones.[34] This is a disadvantage, because their relative intensities must be known and included as overtone coefficients in the data analysis procedure, because they would otherwise result in fake distances.[36]

A different approach for PDS is taken in laser-induced magnetic dipole spectroscopy (LaserIMD).[37,38] Here, the dipolar coupling between a permanent spin label and a label that is transiently converted into a paramagnetic state through photoexcitation is measured. The $\Delta|m_S| = 1$ transition required for PDS is achieved through intersystem crossing from its photoexcited diamagnetic singlet state ($S = 0$) to the paramagnetic triplet state ($S = 1$), thereby replacing the microwave pump pulse used in DEER (Figure 1a). The bandwidth of the photoexcitation is not limited by the EPR spectrum or the microwave resonator and is virtually infinite.[37] Thus, even though such a combination of two distinct labels

Received: July 8, 2022
Accepted: October 3, 2022
Published: November 18, 2022

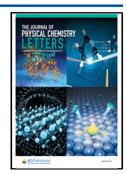

https://doi.org/10.1021/acs.jpclett.2c02138
J. Phys. Chem. Lett. 2022, 13, 10958−10964

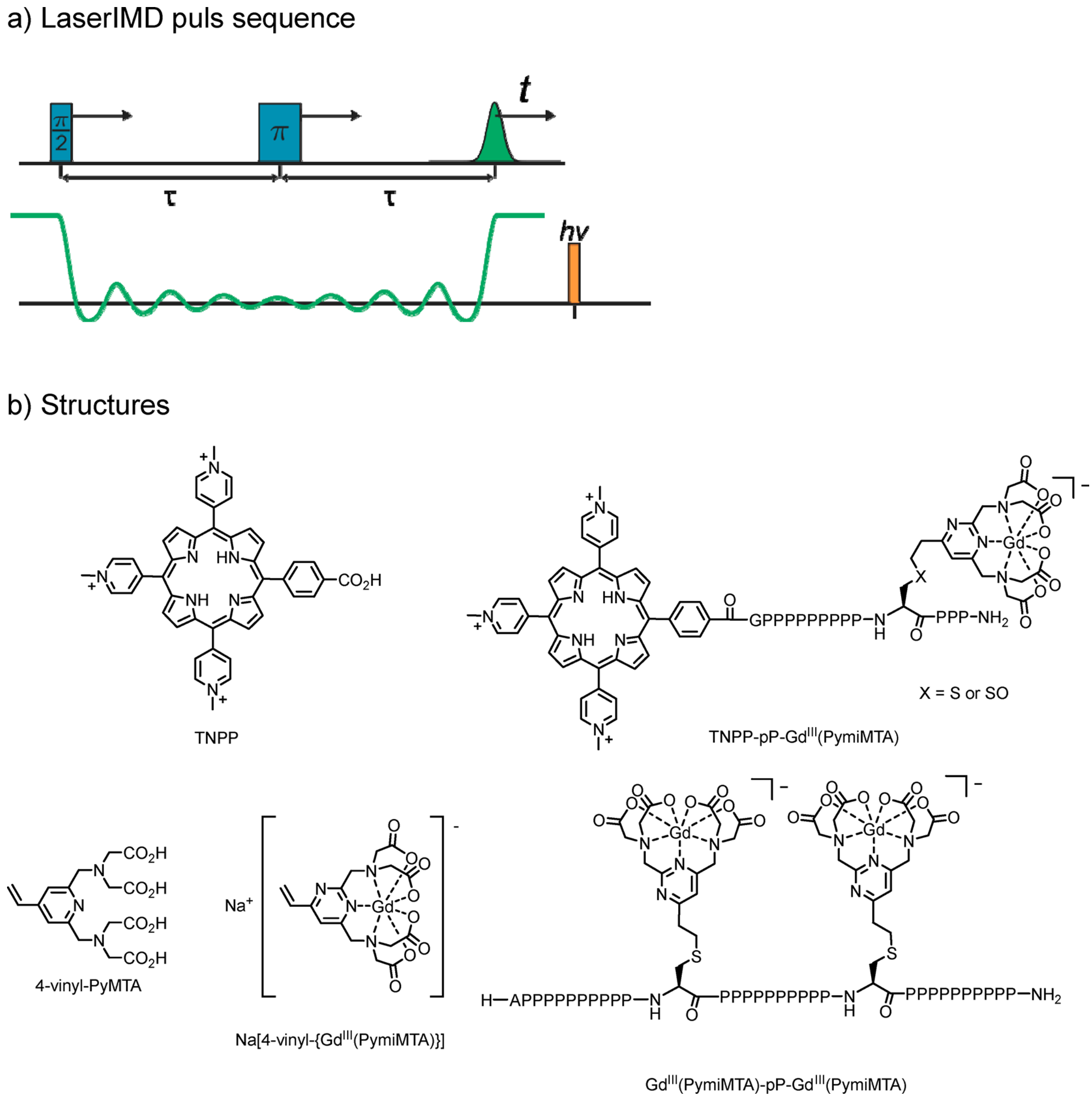

Figure 1. (a) Pulse sequence of LaserIMD. (b) Structural formula of the transient spin label TNPP, the compounds used to install the permanent Gd^{III}-based spin label with PyMTA or PymiMTA as the ligand, and the model peptides TNPP-pP-Gd^{III}(PymiMTA) and Gd^{III}(PymiMTA)-pP-Gd^{III}(PymiMTA). For the peptide chains, the following letter code is used: A, alanine; G, glycine; P, proline.

requires a more difficult labeling scheme for the attachment to a protein,[39,40] LaserIMD on Gd^{III}-based spin labels is a promising technique, because of its potential for achieving higher modulation depths than with $Gd^{III}-Gd^{III}$ DEER. Also, the aforementioned broadening artifacts are avoided in LaserIMD, because only one microwave frequency is used and with a spectral width of 1.5 GHz for the triplet state of the porphyrin, the transient spin label used in this study,[37,41] the frequency offset between pump and observer spins is significantly larger. High modulation depths of over 40% with Gd^{III} spin labels can also be achieved by performing DEER on a nitroxide−Gd^{III} spin pair,[42] However, combining Gd^{III} with a transient spin label instead of a nitroxide has the advantage that photoexcitable groups are endogenous in many proteins like heme-proteins[43] or light-harvesting proteins.[44] In such a case, only a single Gd^{III} label needs to be introduced, which reduces potential disturbances on the protein by the labels.[37] Furthermore, as lanthanide tags have already been shown to be applicable as a FRET donor,[45] the combination of a photoexcitable label and a Gd^{III} label also opens the possibility to combine luminescence-based spectroscopic techniques like Förster resonance energy transfer (FRET) with PDS.

In initial studies of light-induced PDS, porphyrins were paired with nitroxide labels.[37,41] Other label combinations that have been reported since are fullerenes with trityl radicals or nitroxides[46,47] the combination of the fluorescent dyes Rose Bengal, Eosin Y, or Atto Thio12 with a nitroxide[40] and two porphyrins, both of which are photoexcited.[48] We opted for porphyrin as the transient spin label, because of its photostability and selected the porphyrin TNPP (Figure 1) because of its water solubility.[49] Due to the bulkiness of TNPP, it should be considered that upon attachment to a protein it might interfere with the protein structure. For the persistent spin label, we chose Gd^{III}(PymiMTA) (Figure 1)[50,51] which is structurally similar to the well-known Gd^{III}(PyMTA).[21,29,52] The substitution of the pyridine ring for a pyrimidine ring has little effect on the EPR-spectroscopic properties like line width

https://doi.org/10.1021/acs.jpclett.2c02138
J. Phys. Chem. Lett. 2022, 13, 10958−10964

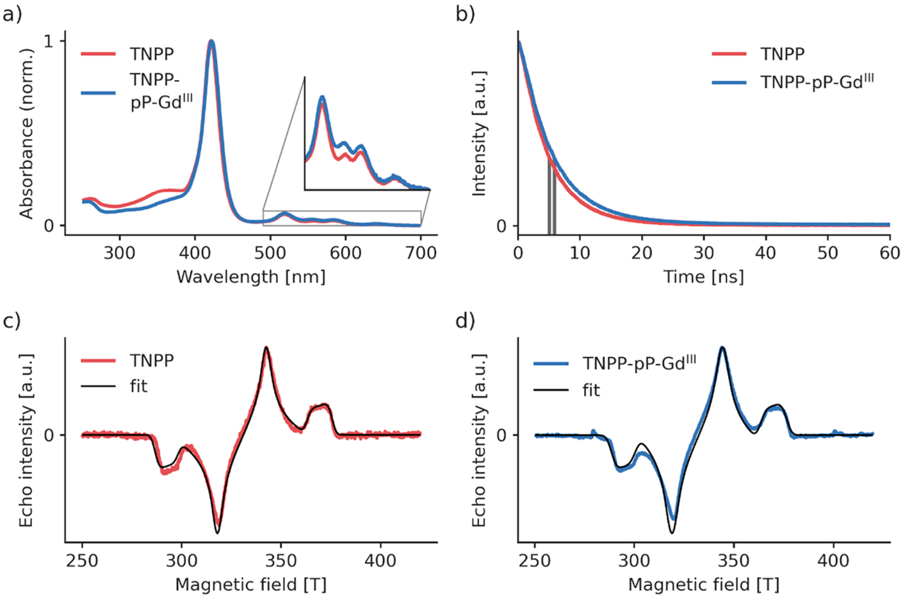

Figure 2. (a) UV/vis spectra of TNPP and TNPP-pP-Gd^{III}(PymiMTA) in water at room temperature. The focused area shows the four Q bands of the TNPP spectrum. (b) Luminescence lifetime measurements of TNPP and TNPP-pP-Gd^{III}(PymiMTA) in water at room temperature with the time points at which the signal intensities have dropped to 1/e. (c) trEPR spectrum of TNPP in D_2O/glycerol-d_8 (40/60 vol %) at 10 K with the corresponding fit (D = 1245 MHz, E = −187 MHz, P_x = 0.26, P_y = 0.59, P_z = 0.15, H_{strain} = 109 MHz). (d) trEPR spectrum of TNPP-pP-Gd^{III}(PymiMTA) in D_2O/glycerol-d_8 (40/60 vol %) at 10 K with the corresponding fit (D = 1227 MHz, E = −172 MHz, P_x = 0.26, P_y = 0.60, P_z = 0.14, H_{strain} = 139 MHz).

and relaxation times, but its bioconjugation rate is much higher.[51]

The combination of a Gd^{III}-based spin label with porphyrin poses potential problems like the incorporation[53,54] of Gd^{III} into the porphyrin or quenching[55−57] of the electronically excited porphyrin by the Gd^{III} complex. Here, we set out to explore this spin label combination, establish LaserIMD with this combination as a light-induced PDS technique and compare its performance with that of Gd^{III}−Gd^{III} DEER.

A model system was designed based on a polyproline helix (pP) as spacer[58,59] between the porphyrin TNPP and Gd^{III}(PymiMTA) (Figure 1b). We attempted to spin label the TNPP-labeled peptide TNPP-GP$_9$CP$_3$−NH$_2$ (G, glycine; P, proline; C, cysteine) with the complex Gd^{III}(PyMTA) by applying a two-step protocol reported for a structurally similar peptide,[21] with first ligand attachment and second complex formation. However, the attachment of 4-vinyl-PyMTA to the cysteine unit of the peptide TNPP-GP$_9$CP$_3$−NH$_2$ failed. Already, in the mentioned previous work, the reaction proceeded rather slowly, even at 40 °C.[21] Turning to Na[4-vinyl-{Gd^{III}(PymiMTA)}] (Figure 1b) as the reaction partner, quantitative spin labeling in a single step was accomplished within 2 h at room temperature. We ascribe the strong increase in reactivity to the increase in electrophility of the vinyl unit after exchanging the pyridine ring for the more electron withdrawing pyrimidine ring. Surprisingly, mass spectrometric analysis of the material, that had been obtained through HPLC, showed a significant amount of sulfoxide linkage (Figure 1, X = SO; Supporting Information, Section S1) alongside the expected sulfide linkage (Figure 1b, X = S). We estimated that the difference between the distance distribution of the sulfoxide and sulfide linkage is negligible and proceeded with the sulfide/sulfoxide mixture. For comparison with Gd^{III}−Gd^{III} DEER, a polyproline helix with two Gd^{III}(PymiMTA) labels (Gd^{III}(PymiMTA)-pP-Gd^{III}(PymiMTA)) was prepared.

Circular dichroism measurements showed that all three peptides adopt a pPII structure in water (Supporting Information, section S2).

For TPP-Gd^{III} LaserIMD it is important that the Gd^{III} ion is not exchanged between the PymiMTA ligand and TNPP.[53,54] An indication of that a metal ion has been incorporated into porphyrin is the change in its UV/vis spectrum from four distinct Q-bands for the metal ion free porphyrin to two Q-bands for the Gd^{III} ion loaded porphyrin.[54] In our case the UV/vis spectrum of TNPP-pP-Gd^{III}(PymiMTA) (Figure 2a, experimental details in Supporting Information, section S3) shows four Q-bands at the same wavelengths as the ion free TNPP, which we take as a strong sign that no Gd^{III} ion exchange took place. This is supported by time-resolved X-band EPR spectra (trEPR) of photoexcited TNPP. Incorporation of a metal ion into porphyrin can significantly change the zero-field splitting and zero-field population of the excited triplet, and hence the trEPR spectrum.[60,61] As can be seen in parts c and d of Figure 2, TNPP-pP-Gd^{III}(PymiMTA) and ion free TNPP show virtually the same trEPR spectrum with almost identical zero-field splitting values and zero-field populations.

Lanthanide cations and their complexes are known to act as photoquenchers of electronically excited states.[55−57] Therefore, the close proximity of Gd^{III}(PymiMTA) to TNPP in TNPP-pP-Gd^{III}(PymiMTA) may quench the photoexcited triplet state, which would interfere with the light-induced PDS measurement and might render it impossible. To check whether quenching takes place, the lifetimes of the excited states of TNPP and TNPP-pP-Gd^{III}(PymiMTA) were determined through time-resolved luminescence measurements at room temperature (experimental details in Supporting Information, section S4). The lifetimes, defined as the time up to which the signal has decayed to 1/e of its maximum value, increases from 5.1 μs for TNPP to 5.9 μs for TNPP-pP-

https://doi.org/10.1021/acs.jpclett.2c02138
J. Phys. Chem. Lett. 2022, 13, 10958−10964

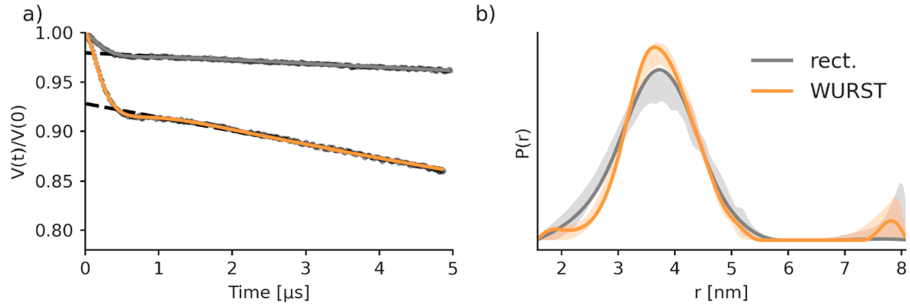

Figure 3. Comparison of Gd^{III}–Gd^{III} DEER data obtained with rectangular and broadband shaped pump pulses from Gd^{III}(PymiMTA)-pP-Gd^{III}(PymiMTA) dissolved in D_2O/glycerol-d_8 (40/60 vol %), at 10 K. (a) Experimentally recorded data and fits. (b) The distance distributions were obtained with Tikhonov regularization.[64]

Gd^{III}(PymiMTA) as can be seen in Figure 2b. Additionally, the average lifetimes of the photoexcited triplet state were determined with pulsed EPR spectroscopy at 10 K (details in Supporting Information, sections S5 and S6).[62] Following the same trend as the luminescence lifetimes, the average triplet lifetimes show an increase from 47.7 ms for TNPP to 57.8 ms for TNPP-pP-Gd^{III}(PymiMTA). Based on these results, we conclude that the photoexcited state of TNPP is not quenched by the close-by Gd^{III}(PymiMTA).

For a fair comparison of TNPP-Gd^{III} LaserIMD and Gd^{III}–Gd^{III} DEER, we first optimized the signal-to-noise ratio (SNR) of the latter by using broadband shaped pulses as pump pulses and fine-tuned the pulse shapes, frequency widths, pulse lengths and observer and pump pulse frequencies.[26] The SNR is calculated as the ratio of the modulation depth and the experimental noise, normalized to the square-root of the measurement time. With the applied optimization heuristic as described in detail in Supporting Information, section S7, the best SNR was obtained when observing at the maximum of the Gd^{III} EPR spectrum at 34 GHz with a Gaussian pulse and pumping with a 200 ns WURST pulse with $n = 12$ and a sweep width of 300 MHz. Gd^{III}–Gd^{III} DEER with these settings on Gd^{III}(PymiMTA)-pP-Gd^{III}(PymiMTA), resulted in a modulation depth of 7.2% and an SNR of 530 $h^{-1/2}$ (Figure 3a and Table 1). Although this is a significantly larger modulation depth than the 2.0% that were reached with a rectangular pump pulse, the modulation depth stays behind what can be achieved with LaserIMD.[41,63]

Table 1. Modulation Depths and SNR for Gd^{III}–Gd^{III} DEER, TNPP-Gd^{III} (re)LaserIMD and TNPP-Gd^{III} reLaserIMD from Figures 3 and 4

	Mod depth [%]	SNR [$h^{-1/2}$]
Gd^{III}–Gd^{III} DEER (WURST, pump pulse)	7.2 (6.9, 7.6)	530 (500, 610)
TNPP-Gd^{III} LaserIMD	39.4 (38.9, 40.1)	190 (180, 210)
TNPP-Gd^{III} reLaserIMD	35.8 (35.3, 36.5)	150 (140, 170)

To prove this, TNPP-Gd^{III} LaserIMD data were recorded at 10 K for TNPP-pP-Gd^{III}(PymiMTA) (results in Figure 4; experimental details in Supporting Information, section S5). The SRT was optimized to 100 ms and the laser energy per pulse to 1.4 mJ (Supporting Information, section S8). If available, temperatures below 10 K can also be used as they are known to give a higher spin-polarization for Gd^{III} in the Q-band.[23] To analyze the dipolar trace, its zero-time needs to be determined precisely. As this cannot always be reliably done for LaserIMD, a LaserIMD experiment with an additional refocusing pulse, termed reLaserIMD, has been suggested as it allows an accurate zero-time determination.[41] However, the introduction of the additional pulse increases the overall trace length which decreases the SNR. To combine the best of both worlds, we tried a different approach where the data were recorded with LaserIMD and then shifted by a zero-time determined with reLaserIMD. As the zero-time does not depend on the dipolar evolution time, the latter can be chosen as short as possible in order to maximize the echo intensity, which allows to record a reLaserIMD trace with a high sensitivity in a short time. Furthermore, for laser systems with a constant delay of the laser flash, the zero-time depends only on the microwave pulse lengths. In such a case, once the zero-time for a given pulse length has been determined, it can be reused for future measurements and it is not necessary to measure reLaserIMD every time. The combination of reLaserIMD and LaserIMD was found to give a reliable zero-time (Supporting Information, section S9) and an SNR increase from 150 $h^{-1/2}$ for TNPP-Gd^{III} reLaserIMD to 190 $h^{-1/2}$ for TNPP-Gd^{III} LaserIMD (Figure 4). The thus optimized TNPP-Gd^{III} LaserIMD gave a modulation depth of 39.4% (Table 1). Even though this stays behind the modulation depth of 50% that has been reported for Gd^{III}–Gd^{III} RIDME,[33] TNPP-Gd^{III} LaserIMD has the advantage, that the laser excites no transitions with $|m_s| > 1$ and therefore no overtones coefficients are needed for data analysis.

The modulation depth of 39% for TNPP-Gd^{III} LaserIMD might be significantly higher than the 7.2% for Gd^{III}–Gd^{III} DEER, but the crucial parameter for the determination of distance distributions is the SNR. Here, TNPP-Gd^{III} LaserIMD has a lower SNR of 190 $h^{-1/2}$ compared to 530 $h^{-1/2}$ for Gd^{III}–Gd^{III} DEER. Due to the short longitudinal relaxation time of Gd^{III}(PymiMTA)-pP-Gd^{III}(PymiMTA) of 35.6 μs (Supporting Information, section S10), it was possible to use a fast shot repetition time (SRT) of 100 μs (Supporting Information, section S7). In contrast, TNPP requires a much longer SRT of 100 ms, because with a triplet relaxation time of 57.8 ms, the signal would saturate otherwise. Therefore, in a given measurement time, Gd^{III}–Gd^{III} DEER benefits from much more scans being accumulated than for TNPP-Gd^{III} LaserIMD, which explains the better SNR of the former. As most transient labels used so far for LaserIMD require an SRT in the millisecond range,[40,46,48,63,65] the continuation of the development of transient spin labels with faster triplet relaxation times is necessary to open up the full possibilities of LaserIMD with Gd^{III}-based spin labels.

https://doi.org/10.1021/acs.jpclett.2c02138
J. Phys. Chem. Lett. 2022, 13, 10958–10964

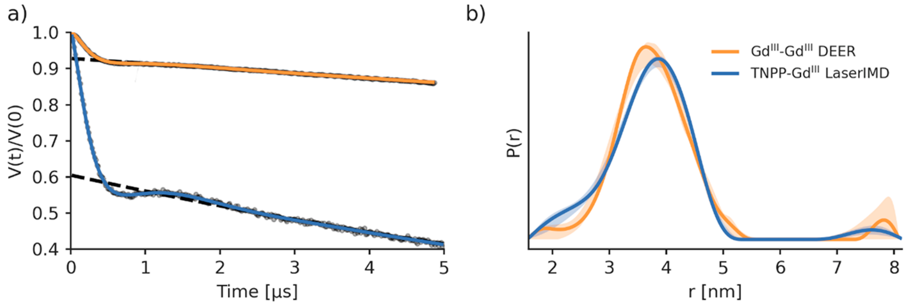

Figure 4. TPP-Gd^{III} LaserIMD and Gd^{III}−Gd^{III} DEER measurements of TNPP-pP-Gd^{III}(PymiMTA) and Gd^{III}(PymiMTA)-pP-Gd^{III}(PymiMTA), respectively, both in D_2O/glycerol-d_8 (40/60 vol %) at 10 K. (a) Experimentally recorded data and fits. (b) The distance distributions were obtained with Tikhonov regularization.[64]

In conclusion, we have shown that TNPP and Gd^{III}(PymiMTA) are a suitable label pair for light-induced EPR measurements and PDS in particular. UV/vis measurements, time-resolved EPR spectroscopy as well as lifetime measurements of the excited TNPP gave neither an indication of a Gd^{III} ion exchange between the labels nor an indication of quenching of the photoexcited triplet state of the TNPP by Gd^{III}−PymiMTA. LaserIMD is an interesting technique, which can be used not just for structural investigations on biological systems with endogenous photoexcitable moieties; the presence of a photoexcitable label also makes it a suitable technique to combine PDS and luminescence measurements. Furthermore, the increase in modulation depth from 7.2% for Gd^{III}−Gd^{III} DEER to 39.7% for TNPP-Gd^{III} LaserIMD promises a significant increase in SNR, once sorter SRTs become applicable.

■ ASSOCIATED CONTENT

Data Availability Statement

The raw data are available at https://doi.org/10.5281/zenodo.7051255.[66]

Supporting Information

The Supporting Information is available free of charge at https://pubs.acs.org/doi/10.1021/acs.jpclett.2c02138.

Synthesis of the model peptides, details on sulfoxide formation and Gd^{III}−Fe^{III} ion exchange, details on CD, UV/vis, fluorescence lifetime, and time-resolved and pumped EPR measurements, MNR optimization of DEER and LaserIMD, zero-time determination for LaserIMD, and and longitudinal and transversal relaxation of Gd^{III} (PDF)

■ AUTHOR INFORMATION

Corresponding Authors

Malte Drescher − *Department of Chemistry and Konstanz Research School Chemical Biology, University of Konstanz, 78457 Konstanz, Germany;* orcid.org/0000-0002-3571-3452; Email: malte.drescher@uni-konstanz.de

Adelheid Godt − *Faculty of Chemistry and Center of Molecular Materials (CM_2), Bielefeld University, 33615 Bielefeld, Germany;* orcid.org/0000-0001-8453-1439; Email: godt@uni-bielefeld.de

Authors

Andreas Scherer − *Department of Chemistry and Konstanz Research School Chemical Biology, University of Konstanz, 78457 Konstanz, Germany;* orcid.org/0000-0002-0708-0686

Xuemei Yao − *Faculty of Chemistry and Center of Molecular Materials (CM_2), Bielefeld University, 33615 Bielefeld, Germany*

Mian Qi − *Faculty of Chemistry and Center of Molecular Materials (CM_2), Bielefeld University, 33615 Bielefeld, Germany*

Max Wiedmaier − *Department of Chemistry and Konstanz Research School Chemical Biology, University of Konstanz, 78457 Konstanz, Germany*

Complete contact information is available at: https://pubs.acs.org/10.1021/acs.jpclett.2c02138

Notes

The authors declare no competing financial interest.

■ ACKNOWLEDGMENTS

We thank Jörg Wolfram Anselm Fischer for support with the time-resolved EPR measurements and Michael Linseis for support with the luminescence lifetimes measurements. Stephan Pritz from Biosynthan, Sonja Tischlik, and Dennis Bücker are thanked for helpful discussions. This project has received funding from the European Research Council (ERC) under the European Union's Horizon 2020 research and innovation program (Grant Agreement Number: 772027-SPICE-ERC-2017-COG). A. Scherer gratefully acknowledges financial support from the Konstanz Research School Chemical Biology (KoRS-CB). X. Yao expresses thanks for a Ph.D. fellowship from the China Scholarship Council (CSC).

■ REFERENCES

(1) Pannier, M.; Veit, S.; Godt, A.; Jeschke, G.; Spiess, H. W. Dead-Time Free Measurement of Dipole−Dipole Interactions between Electron Spins. *J. Magn. Reson.* **2000**, *142*, 331−340.

(2) Yee, E. F.; Diensthuber, R. P.; Vaidya, A. T.; Borbat, P. P.; Engelhard, C.; Freed, J. H.; Bittl, R.; Möglich, A.; Crane, B. R. Signal Transduction in Light−Oxygen−Voltage Receptors Lacking the Adduct-Forming Cysteine Residue. *Nat. Commun.* **2015**, *6*, 10079.

(3) Yang, Y.; Chen, S.-N.; Yang, F.; Li, X.-Y.; Feintuch, A.; Su, X.-C.; Goldfarb, D. In-Cell Destabilization of a Homodimeric Protein Complex Detected by DEER Spectroscopy. *Proc. Natl. Acad. Sci. U. S. A.* **2020**, *117*, 20566.

(4) Giannoulis, A.; Feintuch, A.; Barak, Y.; Mazal, H.; Albeck, S.; Unger, T.; Yang, F.; Su, X.-C.; Goldfarb, D. Two Closed ATP- and ADP-Dependent Conformations in Yeast Hsp90 Chaperone Detected by Mn(II) EPR Spectroscopic Techniques. *Proc. Natl. Acad. Sci. U. S. A.* **2020**, *117*, 395.

(5) Weickert, S.; Wawrzyniuk, M.; John, L. H.; Rüdiger, S. G. D.; Drescher, M. The Mechanism of Hsp90-Induced Oligomerizaton of Tau. *Sci. Adv.* **2020**, *6*, No. eaax6999.

(6) Wojciechowski, F.; Groß, A.; Holder, I. T.; Knörr, L.; Drescher, M.; Hartig, J. S. Pulsed EPR Spectroscopy Distance Measurements of DNA Internally Labelled with Gd3+-DOTA. *Chem. Commun.* **2015**, *51*, 13850−13853.

(7) Ghosh, S.; Casto, J.; Bogetti, X.; Arora, C.; Wang, J.; Saxena, S. Orientation and Dynamics of Cu2+ Based DNA Labels from Force Field Parameterized MD Elucidates the Relationship between EPR Distance Constraints and DNA Backbone Distances. *Phys. Chem. Chem. Phys.* **2020**, *22*, 26707−26719.

(8) Collauto, A.; von Bülow, S.; Gophane, D. B.; Saha, S.; Stelzl, L. S.; Hummer, G.; Sigurdsson, S. T.; Prisner, T. F. Compaction of RNA Duplexes in the Cell. *Angew. Chem., Int. Ed.* **2020**, *59*, 23025.

(9) Schiemann, O.; Heubach, C. A.; Abdullin, D.; Ackermann, K.; Azarkh, M.; Bagryanskaya, E. G.; Drescher, M.; Endeward, B.; Freed, J. H.; Galazzo, L.; Goldfarb, D.; Hett, T.; Esteban Hofer, L.; Fábregas Ibáñez, L.; Hustedt, E. J.; Kucher, S.; Kuprov, I.; Lovett, J. E.; Meyer, A.; Ruthstein, S.; Saxena, S.; Stoll, S.; Timmel, C. R.; Di Valentin, M.; Mchaourab, H. S.; Prisner, T. F.; Bode, B. E.; Bordignon, E.; Bennati, M.; Jeschke, G. Benchmark Test and Guidelines for DEER/PELDOR Experiments on Nitroxide-Labeled Biomolecules. *J. Am. Chem. Soc.* **2021**, *143*, 17875−17890.

(10) Kurshev, V. V.; Raitsimring, A. M.; Tsvetkov, Y. D. Selection of Dipolar Interaction by the "2 + 1" Pulse Train ESE. *Journal of Magnetic Resonance (1969)* **1989**, *81*, 441−454.

(11) Jeschke, G.; Pannier, M.; Godt, A.; Spiess, H. W. Dipolar Spectroscopy and Spin Alignment in Electron Paramagnetic Resonance. *Chem. Phys. Lett.* **2000**, *331*, 243−252.

(12) Milikisyants, S.; Scarpelli, F.; Finiguerra, M. G.; Ubbink, M.; Huber, M. A Pulsed EPR Method to Determine Distances between Paramagnetic Centers with Strong Spectral Anisotropy and Radicals: The Dead-Time Free RIDME Sequence. *J. Magn. Reson.* **2009**, *201*, 48−56.

(13) Borbat, P. P.; Freed, J. H. Multiple-Quantum ESR and Distance Measurements. *Chem. Phys. Lett.* **1999**, *313*, 145−154.

(14) Jeschke, G. DEER Distance Measurements on Proteins. *Annu. Rev. Phys. Chem.* **2012**, *63*, 419−446.

(15) Kugele, A.; Silkenath, B.; Langer, J.; Wittmann, V.; Drescher, M. Protein Spin Labeling with a Photocaged Nitroxide Using Diels-Alder Chemistry. *ChemBioChem.* **2019**, *20*, 2479.

(16) Widder, P.; Berner, F.; Summerer, D.; Drescher, M. Double Nitroxide Labeling by Copper-Catalyzed Azide−Alkyne Cycloadditions with Noncanonical Amino Acids for Electron Paramagnetic Resonance Spectroscopy. *ACS Chem. Biol.* **2019**, *14*, 839−844.

(17) Bleicken, S.; Assafa, T. E.; Zhang, H.; Elsner, C.; Ritsch, I.; Pink, M.; Rajca, S.; Jeschke, G.; Rajca, A.; Bordignon, E. Gem-Diethyl Pyrroline Nitroxide Spin Labels: Synthesis, EPR Characterization, Rotamer Libraries and Biocompatibility. *ChemistryOpen* **2019**, *8*, 1035.

(18) Fleck, N.; Heubach, C.; Hett, T.; Spicher, S.; Grimme, S.; Schiemann, O. Ox-SLIM: Synthesis of and Site-Specific Labelling with a Highly Hydrophilic Trityl Spin Label. *Chemistry A European Journal* **2021**, *27*, 5292.

(19) Theillet, F.-X.; Binolfi, A.; Bekei, B.; Martorana, A.; Rose, H. M.; Stuiver, M.; Verzini, S.; Lorenz, D.; van Rossum, M.; Goldfarb, D.; Selenko, P. Structural Disorder of Monomeric α-Synuclein Persists in Mammalian Cells. *Nature* **2016**, *530*, 45.

(20) Kucher, S.; Korneev, S.; Klare, J. P.; Klose, D.; Steinhoff, H.-J. In Cell Gd3+-Based Site-Directed Spin Labeling and EPR Spectroscopy of EGFP. *Phys. Chem. Chem. Phys.* **2020**, *22*, 13358.

(21) Qi, M.; Groß, A.; Jeschke, G.; Godt, A.; Drescher, M. Gd(III)-PyMTA Label Is Suitable for In-Cell EPR. *J. Am. Chem. Soc.* **2014**, *136*, 15366−15378.

(22) Martorana, A.; Bellapadrona, G.; Feintuch, A.; Di Gregorio, E.; Aime, S.; Goldfarb, D. Probing Protein Conformation in Cells by EPR Distance Measurements Using Gd3+ Spin Labeling. *J. Am. Chem. Soc.* **2014**, *136*, 13458−13465.

(23) Goldfarb, D. Gd3+ Spin Labeling for Distance Measurements by Pulse EPR Spectroscopy. *Phys. Chem. Chem. Phys.* **2014**, *16*, 9685−9699.

(24) Bahrenberg, T.; Rosenski, Y.; Carmieli, R.; Zibzener, K.; Qi, M.; Frydman, V.; Godt, A.; Goldfarb, D.; Feintuch, A. Improved Sensitivity for W-Band Gd(III)-Gd(III) and Nitroxide-Nitroxide DEER Measurements with Shaped Pulses. *J. Magn. Reson.* **2017**, *283*, 1−13.

(25) Doll, A.; Qi, M.; Pribitzer, S.; Wili, N.; Yulikov, M.; Godt, A.; Jeschke, G. Sensitivity Enhancement by Population Transfer in Gd(Iii) Spin Labels. *Phys. Chem. Chem. Phys.* **2015**, *17*, 7334−7344.

(26) Doll, A.; Qi, M.; Wili, N.; Pribitzer, S.; Godt, A.; Jeschke, G. Gd(III)−Gd(III) Distance Measurements with Chirp Pump Pulses. *J. Magn. Reson.* **2015**, *259*, 153−162.

(27) Feintuch, A.; Otting, G.; Goldfarb, D. Chapter Sixteen - Gd3+ Spin Labeling for Measuring Distances in Biomacromolecules: Why and How? In *Methods in Enzymology*; Qin, P. Z., Warncke, K., Eds.; Academic Press: 2015; Vol. *563*, pp 415−457.

(28) Clayton, J. A.; Keller, K.; Qi, M.; Wegner, J.; Koch, V.; Hintz, H.; Godt, A.; Han, S.; Jeschke, G.; Sherwin, M. S.; et al. Quantitative Analysis of Zero-Field Splitting Parameter Distributions in Gd (Iii) Complexes. *Phys. Chem. Chem. Phys.* **2018**, *20*, 10470−10492.

(29) Dalaloyan, A.; Qi, M.; Ruthstein, S.; Vega, S.; Godt, A.; Feintuch, A.; Goldfarb, D. Gd(Iii)-Gd(Iii) EPR Distance Measurements - the Range of Accessible Distances and the Impact of Zero Field Splitting. *Phys. Chem. Chem. Phys.* **2015**, *17*, 18464−18476.

(30) Manukovsky, N.; Feintuch, A.; Kuprov, I.; Goldfarb, D. Time Domain Simulation of Gd3+−Gd3+ Distance Measurements by EPR. *J. Chem. Phys.* **2017**, *147*, 044201.

(31) Cohen, M. R.; Frydman, V.; Milko, P.; Iron, M. A.; Abdelkader, E. H.; Lee, M. D.; Swarbrick, J. D.; Raitsimring, A.; Otting, G.; Graham, B.; Feintuch, A.; Goldfarb, D. Overcoming Artificial Broadening in Gd3+−Gd3+ Distance Distributions Arising from Dipolar Pseudo-Secular Terms in DEER Experiments. *Phys. Chem. Chem. Phys.* **2016**, *18*, 12847−12859.

(32) EL Mkami, H.; Hunter, R. I.; Cruickshank, P. A. S.; Taylor, M. J.; Lovett, J. E.; Feintuch, A.; Qi, M.; Godt, A.; Smith, G. M. High-Sensitivity Gd3+−Gd3+ EPR Distance Measurements That Eliminate Artefacts Seen at Short Distances. *Magn. Reson.* **2020**, *1*, 301−313.

(33) Razzaghi, S.; Qi, M.; Nalepa, A. I.; Godt, A.; Jeschke, G.; Savitsky, A.; Yulikov, M. RIDME Spectroscopy with Gd(III) Centers. *J. Phys. Chem. Lett.* **2014**, *5*, 3970−3975.

(34) Collauto, A.; Frydman, V.; Lee, M.; Abdelkader, E.; Feintuch, A.; Swarbrick, J.; Graham, B.; Otting, G.; Goldfarb, D. RIDME Distance Measurements Using Gd (Iii) Tags with a Narrow Central Transition. *Phys. Chem. Chem. Phys.* **2016**, *18*, 19037−19049.

(35) Kulik, L. V.; Dzuba, S. A.; Grigoryev, I. A.; Tsvetkov, Yu. D. Electron Dipole−Dipole Interaction in ESEEM of Nitroxide Biradicals. *Chem. Phys. Lett.* **2001**, *343*, 315−324.

(36) Keller, K.; Mertens, V.; Qi, M.; Nalepa, A. I.; Godt, A.; Savitsky, A.; Jeschke, G.; Yulikov, M. Computing Distance Distributions from Dipolar Evolution Data with Overtones: RIDME Spectroscopy with Gd(Iii)-Based Spin Labels. *Phys. Chem. Chem. Phys.* **2017**, *19*, 17856−17876.

(37) Hintze, C.; Bücker, D.; Domingo Köhler, S.; Jeschke, G.; Drescher, M. Laser-Induced Magnetic Dipole Spectroscopy. *J. Phys. Chem. Lett.* **2016**, *7*, 2204−2209.

(38) Bertran, A.; Barbon, A.; Bowen, A. M.; Di Valentin, M. Chapter Seven - Light-Induced Pulsed Dipolar EPR Spectroscopy for Distance and Orientation Analysis. In *Methods in Enzymology*; Britt, R. D., Ed.; Academic Press: 2022; Vol. *666*, pp 171−231.

(39) Gmeiner, C.; Klose, D.; Mileo, E.; Belle, V.; Marque, S. R. A.; Dorn, G.; Allain, F. H. T.; Guigliarelli, B.; Jeschke, G.; Yulikov, M. Orthogonal Tyrosine and Cysteine Site-Directed Spin Labeling for Dipolar Pulse EPR Spectroscopy on Proteins. *J. Phys. Chem. Lett.* **2017**, *8*, 4852−4857.

(40) Williams, L.; Tischlik, S.; Scherer, A.; Fischer, J. W. A.; Drescher, M. Site-Directed Attachment of Photoexcitable Spin Labels

for Light-Induced Pulsed Dipolar Spectroscopy. *Chem. Commun.* **2020**, *56*, 14669−14672.
(41) Dal Farra, M. G.; Richert, S.; Martin, C.; Larminie, C.; Gobbo, M.; Bergantino, E.; Timmel, C. R.; Bowen, A. M.; Di Valentin, M. Light-Induced Pulsed EPR Dipolar Spectroscopy on a Paradigmatic Hemeprotein. *ChemPhysChem* **2019**, *20*, 931.
(42) Garbuio, L.; Bordignon, E.; Brooks, E. K.; Hubbell, W. L.; Jeschke, G.; Yulikov, M. Orthogonal Spin Labeling and Gd(III)−Nitroxide Distance Measurements on Bacteriophage T4-Lysozyme. *J. Phys. Chem. B* **2013**, *117*, 3145−3153.
(43) Reedy, C. J.; Gibney, B. R. Heme Protein Assemblies. *Chem. Rev.* **2004**, *104*, 617−650.
(44) Büchel, C. Evolution and Function of Light Harvesting Proteins. *Journal of Plant Physiology* **2015**, *172*, 62−75.
(45) Herath, I.; Breen, C.; Hewitt, S.; Berki, T.; Kassir, A.; Dodson, C.; Judd, M.; Jabar, S.; Cox, N.; Otting, G.; Butler, S. J. A Chiral Lanthanide Tag for Stable and Rigid Attachment to Single Cysteine Residues in Proteins for NMR, EPR and Time-Resolved Luminescence Studies. *Chemistry A European Journal* **2021**, *27*, 13009.
(46) Timofeev, I. O.; Politanskaya, L. V.; Tretyakov, E. V.; Polienko, Y. F.; Tormyshev, V. M.; Bagryanskaya, E.; Krumkacheva, O. A.; Fedin, M. V. Fullerene-Based Triplet Spin Labels: Methodology Aspects for Pulsed Dipolar EPR Spectroscopy. *Phys. Chem. Chem. Phys.* **2022**, *24*, 4475−4484.
(47) Krumkacheva, O. A.; Timofeev, I. O.; Politanskaya, L. V.; Polienko, Y. F.; Tretyakov, E. V.; Rogozhnikova, O. Yu.; Trukhin, D. V.; Tormyshev, V. M.; Chubarov, A. S.; Bagryanskaya, E. G.; Fedin, M. V. Triplet Fullerenes as Prospective Spin Labels for Nanoscale Distance Measurements by Pulsed Dipolar EPR. *Angew. Chem.* **2019**, *131*, 13405.
(48) Bertran, A.; Henbest, K. B.; De Zotti, M.; Gobbo, M.; Timmel, C. R.; Di Valentin, M.; Bowen, A. M. Light-Induced Triplet−Triplet Electron Resonance Spectroscopy. *J. Phys. Chem. Lett.* **2021**, *12*, 80−85.
(49) Sannikova, N.; Timofeev, I.; Bagryanskaya, E.; Bowman, M.; Fedin, M.; Krumkacheva, O. Electron Spin Relaxation of Photoexcited Porphyrin in Water—Glycerol Glass. *Molecules* **2020**, *25*, 2677.
(50) Keller, K. *Metal Centres in Pulsed Dipolar Spectroscopy−From Methodology to Application*. 2019.
(51) Yao, X. *Promotionsarbeit Universität Bielefeld*. 2019.
(52) Yang, Y.; Wang, J.-T.; Pei, Y.-Y.; Su, X.-C. Site-Specific Tagging Proteins via a Rigid, Stable and Short Thiolether Tether for Paramagnetic Spectroscopic Analysis. *Chem. Commun.* **2015**, *51*, 2824−2827.
(53) Zang, L.; Zhao, H.; Zheng, Y.; Qin, F.; Yao, J.; Tian, Y.; Zhang, Z.; Cao, W. Twenty-Fold Enhancement of Gadolinium-Porphyrin Phosphorescence at Room Temperature by Free Gadolinium Ion in Liquid Phase. *J. Phys. Chem. C* **2015**, *119*, 28111−28116.
(54) Zang, L.; Zhao, H.; Hua, J.; Qin, F.; Zheng, Y.; Zhang, Z.; Cao, W. Water-Soluble Gadolinium Porphyrin as a Multifunctional Theranostic Agent: Phosphorescence-Based Oxygen Sensing and Photosensitivity. *Dyes Pigm.* **2017**, *142*, 465−471.
(55) Buono-core, G. E.; Li, H.; Marciniak, B. Quenching of Excited States by Lanthanide Ions and Chelates in Solution. *Coord. Chem. Rev.* **1990**, *99*, 55−87.
(56) Lis, S.; Elbanowski, M.; Mąkowska, B.; Hnatejko, Z. Energy Transfer in Solution of Lanthanide Complexes. *J. Photochem. Photobiol., A* **2002**, *150*, 233−247.
(57) Li, J.; Wang, Y.; Jiang, X.; Wu, P. An Aqueous Room-Temperature Phosphorescent Probe for Gd3+. *Chem. Commun.* **2022**, *58*, 2686−2689.
(58) Stryer, L.; Haugland, R. P. Energy Transfer: A Spectroscopic Ruler. *Proc. Natl. Acad. Sci. U. S. A.* **1967**, *58*, 719−726.
(59) Garbuio, L.; Lewandowski, B.; Wilhelm, P.; Ziegler, L.; Yulikov, M.; Wennemers, H.; Jeschke, G. Shape Persistence of Polyproline II Helical Oligoprolines. *Chemistry A European Journal* **2015**, *21*, 10747−10753.
(60) Ishii, K.; Fujisawa, J.; Ohba, Y.; Yamauchi, S. A Time-Resolved Electron Paramagnetic Resonance Study on the Excited States of Tetraphenylporphinatozinc(II) Coordinated by p-Pyridyl Nitronyl Nitroxide. *J. Am. Chem. Soc.* **1996**, *118*, 13079.
(61) Tait, C. E.; Neuhaus, P.; Peeks, M. D.; Anderson, H. L.; Timmel, C. R. Transient EPR Reveals Triplet State Delocalization in a Series of Cyclic and Linear π-Conjugated Porphyrin Oligomers. *J. Am. Chem. Soc.* **2015**, *137*, 8284−8293.
(62) Hintze, C.; Morgen, T. O.; Drescher, M. Heavy-Atom Effect on Optically Excited Triplet State Kinetics. *PLoS One* **2017**, *12*, No. e0184239.
(63) Bieber, A.; Bücker, D.; Drescher, M. Light-Induced Dipolar Spectroscopy − A Quantitative Comparison between LiDEER and LaserIMD. *J. Magn. Reson.* **2018**, *296*, 29−35.
(64) Fábregas Ibáñez, L.; Jeschke, G.; Stoll, S. DeerLab: A Comprehensive Toolbox for Analyzing Dipolar EPR Spectroscopy Data. *Magn. Reson.* **2020**, *1*, 209.
(65) Di Valentin, M.; Albertini, M.; Zurlo, E.; Gobbo, M.; Carbonera, D. Porphyrin Triplet State as a Potential Spin Label for Nanometer Distance Measurements by PELDOR Spectroscopy. *J. Am. Chem. Soc.* **2014**, *136*, 6582−6585.
(66) Scherer, A.; Yao, X.; Qi, M.; Wiedmaier, M.; Godt, A.; Drescher, M. Raw Data for "Increasing the Modulation Depth of Gd(III)-Based Pulsed Dipolar EPR Spectroscopy (PDS) with Porphyrin-GdIII Laser Induced Magnetic Dipole Spectroscopy. *Zenodo* 2022. DOI: 10.5281/zenodo.7051255

https://doi.org/10.1021/acs.jpclett.2c02138
J. Phys. Chem. Lett. 2022, 13, 10958−10964